Original article

MOLECULAR METABOLISM

Sphingosine kinase 2 and p62 regulation are determinants of sexual dimorphism in hepatocellular carcinoma

Christopher D. Green[1,*], Ryan D.R. Brown[1], Baasanjav Uranbileg[2], Cynthia Weigel[1], Sumit Saha[1], Makoto Kurano[2,3], Yutaka Yatomi[2,3], Sarah Spiegel[1]

ABSTRACT

Objective: Hepatocellular carcinoma (HCC) is the third leading cause of cancer mortality, and its incidence is increasing due to endemic obesity. HCC is sexually dimorphic in both humans and rodents with higher incidence in males, although the mechanisms contributing to these correlations remain unclear. Here, we examined the role of sphingosine kinase 2 (SphK2), the enzyme that regulates the balance of bioactive sphingolipid metabolites, sphingosine-1-phosphate (S1P) and ceramide, in gender specific MASH-driven HCC.

Methods: Male and female mice were fed a high fat diet with sugar water, a clinically relevant model that recapitulates MASH-driven HCC in humans followed by physiological, biochemical cellular and molecular analyses. In addition, correlations with increased risk of HCC recurrence were determined in patients.

Results: Here, we report that deletion of SphK2 protects both male and female mice from Western diet-induced weight gain and metabolic dysfunction without affecting hepatic lipid accumulation or fibrosis. However, SphK2 deficiency decreases chronic diet-induced hepatocyte proliferation in males but increases it in females. Remarkably, SphK2 deficiency reverses the sexual dimorphism of HCC, as SphK2$^{-/-}$ male mice are protected whereas the females develop liver cancer. Only in male mice, chronic western diet induced accumulation of the autophagy receptor p62 and its downstream mediators, the antioxidant response target NQO1, and the oncogene c-Myc. SphK2 deletion repressed these known drivers of HCC development. Moreover, high p62 expression correlates with poor survival in male HCC patients but not in females. In hepatocytes, lipotoxicity-induced p62 accumulation is regulated by sex hormones and prevented by SphK2 deletion. Importantly, high SphK2 expression in male but not female HCC patients is associated with a more aggressive HCC differentiation status and increased risk of cancer recurrence.

Conclusions: This work identifies SphK2 as a potential regulator of HCC sexual dimorphism and suggests SphK2 inhibitors now in clinical trials could have opposing, gender-specific effects in patients.

Keywords Hepatocellular carcinoma; Obesity; Sphingosine kinase; Sexual dimorphism; Metabolic dysfunction-associated steatohepatitis

1. INTRODUCTION

Hepatocellular carcinoma (HCC) is the third leading cause of cancer-related deaths worldwide and its incidence is increasing due to the global obesity crisis [1]. Sexual dimorphism exists in HCC incidence as women have a significantly lower risk for developing HCC than men [1,2]. Similarly, female rodents are resistant to carcinogen- and diet-induced liver cancer [3]. This disparity in HCC incidence in humans and mice has been linked to sex-specific factors including differential hepatocyte transcription, regulation of cell cycle/proliferation and detoxification genes by sex hormones, mitochondrial function, and inflammatory responses [2,4]. Moreover, genetic alterations of chromosomes X and Y are frequently observed in patients with HCC [2]. Nevertheless, the mechanism for sexual dimorphism in HCC remains unclear and may be dependent on specific etiologies of liver cancer.

The main etiologies of HCC include hepatitis B virus (HBV) and hepatitis C virus (HCV) infections, excessive alcohol consumption, and a progressive form of Metabolic-Associated Fatty Liver Disease (MAFLD) termed Metabolic-Associated Steatohepatitis (MASH). While mortality rates caused by HBV and HCV are decreasing, the growing prevalence of MAFLD, often linked with metabolic syndrome and obesity, is emerging as a prominent contributor to liver cancer in the Western world [1].

Obesity-related MASH is characterized by gradual progression from liver steatosis to hepatocellular injury/ballooning, inflammatory cell infiltration, and pericellular fibrosis that predisposes individuals to developing HCC [5]. In preclinical models of MASH-driven HCC, molecular analyses have identified key genes and pathways related to inflammation, endoplasmic reticulum and oxidative stress, and accumulation of the autophagy receptor p62 that permits transition of premalignant hepatocytes to liver cancer that are involved in the

[1]Department of Biochemistry and Molecular Biology, Virginia Commonwealth University School of Medicine, Richmond, VA, USA [2]Department of Clinical Laboratory Medicine, The University of Tokyo, Tokyo, Japan [3]CREST, JST, Japan

*Corresponding author. E-mail: christopher.d.green@vcuhealth.org (C.D. Green).

Received April 13, 2024 • Revision received June 16, 2024 • Accepted June 18, 2024 • Available online 24 June 2024

https://doi.org/10.1016/j.molmet.2024.101971

pathogenesis of this disease [3,6]. Recently, Western diet (WD) based mouse models were developed that mimic the gradual progression of steatosis to MASH and HCC as well as the key physiological, metabolic, and histologic changes and sexual dimorphism observed in the human disease [3,7]. Despite these advances, the mechanisms of sex differences for this etiology are still not understood.

The bioactive sphingolipid metabolites sphingosine-1-phosphate (S1P) and ceramide accumulate with overnutrition and have been implicated in MAFLD/MASH [8] and HCC [9]. S1P generated by one of the sphingosine kinases, SphK1, correlates with poor prognosis in patients [10] and contributes to hepatocarcinogenesis in mice [9]. Moreover, loss of SphK1 in hepatocytes exacerbated deposition of liver collagen in a mouse model of MAFLD in a sex-dependent manner [11]. Very little is known about the role of the other isoenzyme SphK2 in HCC, and reports of SphK2 involvement in liver function have been inconsistent [12–18]. SphK2$^{-/-}$ knockout mice were shown to be protected from HFD-induced diabetes and age-related obesity and development of fatty liver [14,15]. Conversely, another report showed that short term HFD feeding enhanced steatosis in SphK2$^{-/-}$ mice [12], and hepatic overexpression of SphK2 improved steatosis and insulin resistance in male mice [13]. Moreover, previous SphK2 studies used mouse diet models [12,14–16] that do not develop the known hallmarks of the progression of MASH to HCC in humans. As only male mice were used in these studies, the potential contribution of SphK2 to the sexual dimorphism of MASH-driven HCC has not yet been explored. Although the SphK2 inhibitor ABC294640 (Opaganib/Yeliva) reduced growth of HCC xenografts [19], and was tested in a phase I clinical trial for treatment of HCC patients (NCT01488513), its gender-specific anti-tumor efficacy has not been evaluated. Furthermore, it was reported that ABC294640 has antiestrogenic effects [20] and metabolic profiling revealed SphK2 as a key target of (phyto)estrogen action [21].

Here, to examine the role of SphK2 in gender-specific MASH-driven HCC, male and female mice were fed western diet (WD), a clinically relevant model that we have shown mimics the gradual progression, histopathology, and molecular signatures of the human disease [7]. We found that SphK2 deletion improved WD-mediated metabolic dysfunction in both males and females. Strikingly, SphK2$^{-/-}$ males had reduced tumor incidence, whereas in females, liver cancer developed only in SphK2$^{-/-}$ mice. We further showed that only in males SphK2 regulates p62, a known driver of HCC [6]. In human patients, we found increased expression of SphK2 in hepatic tumors and that higher SphK2 expression was associated with increased risk for recurrence of cancer after resection in males, but not in females. Our findings suggest that sexually dimorphic HCC is dependent on SphK2, which could affect treatment regimens with SphK2 inhibitors in the clinic.

2. MATERIALS AND METHODS

2.1. Animals

All animal procedures conducted were approved by the Institutional Animal Care and Use Committee of Virginia Commonwealth University. Wild-type (WT) and SphK2$^{-/-}$ mice on the C57BL/6NJ background were purchased from Jackson Laboratory (Bar Harbor) and maintained by heterozygous SphK2$^{+/-}$ inbreeding. Mice were housed in a 12 h light/dark cycle in a 21–23 °C animal care facility at Virginia Commonwealth University and maintained on standard chow diet (Harlan TD.7912; Envigo). Mice aged 8–9 weeks were randomly assigned to be fed *ad libitum* chow diet (CD) and provided normal drinking water or fed a Western diet (WD) high in fat (42% kcal from milk fat), cholesterol (0.2%), and sucrose-enriched carbohydrates (42.7% kcal) (Harlan TD.88137; Envigo) plus drinking water supplemented with high D-fructose (23.1 g/L) and D-glucose (18.9 g/L).

2.2. Human autophagy-related gene analysis

Tumor mRNA expression values for 62 autophagy-related genes previously found differentially expressed in tumors compared to non-tumors [22] and *NQO1* were obtained from cBioPortal analysis [23] of The Cancer Genome Atlas (TCGA) PanCancer Atlas data for 120 female and 246 male patients with HCC. Values are expressed as z-score normalized mRNA expression of tumor samples relative to the expression distribution of all log-transformed mRNA expression of adjacent normal samples.

2.3. Kaplan–Meier survival curve analysis

Ten-year overall survival data for male and female patients with HCC were obtained from cBioPortal. Patients were stratified by *SQSTM1* or *NQO1* tumor mRNA levels (z-score normalized relative to adjacent normal samples) from the TCGA PanCancer Atlas, comparing patients with mRNA z-scores >2 (males and females) for *SQSTM1* and z-scores >3.5 (males) or 2.5 (females) for *NQO1* relative to the remaining patients. Similarly, Kaplan–Meier curve analyses were performed for the cumulative incidence of intra- and extra-hepatic recurrence. Survival data for the respective groups was plotted with GraphPad Prism and analyzed by the logrank test.

2.4. Human *SPHK2* expression from TCGA

Human SphK2 expression from non-tumor and tumor samples in the TCGA was analyzed using the University of ALabama at Birmingham CANcer data analysis Portal (UALCAN) [24,25].

2.5. Human patient samples

Tumor and adjacent non-tumor samples were obtained from 148 patients with HCC and treated at the Hepatobiliary Pancreatic Surgery Division, Department of Surgery, at the University of Tokyo Hospital. Liver resection was performed on all the enrolled patients [26]. Patients with primary HCC were followed-up to evaluate intra- and extra-hepatic HCC recurrence after surgical treatment. This study was conducted with the approval of the Institutional Research Ethics Committee of the University of Tokyo (Approval number 1143-2). Written informed consent was obtained from the patients for the use of their clinical samples [26].

2.6. Tissue and blood analysis

Mice at the indicated timepoints of dietary treatments were weighed and euthanized with 5% isoflurane. Whole blood was collected by cardiac puncture, transferred to BD Microtaine Capillary Blood Collector tubes (Thermo Fisher, 02-675-185) and centrifuged after 30 min to collect serum. Livers and gonadal epididymal white adipose tissues (eWAT) were removed. Tumors were measured using a caliper and tumor volumes determined using formula $V = (W^2 \times L)/2$, where V is the tumor volume, W is the tumor width, and L is the tumor length. Tissues were snap frozen in liquid nitrogen or in Tissue-Tek optimal cutting temperature solution or fixed in 10% neutral buffered formalin (Thermo Fisher, #245684) and embedded in paraffin. Alanine aminotransferase (ALT) and Aspartate aminotransferase (AST) levels were measured using the Cobas ALTL and ASTL kits with a Cobas c311 Analyzer (Roche Diagnostics).

2.7. Glucose tolerance test

After an overnight fast, baseline blood glucose levels were determined from tail-vein blood using a TRUEtrack Blood Glucose meter (Nipro

Diagnostics, B0727V3XQX) and test strips (Amazon, B01M8KJG0A). Glucose (2 mg dextrose/g body weight) was dissolved in sterile PBS and injected intraperitoneally. Blood glucose levels were measured at 15, 30, 60, 90, and 120 min after glucose injection, and areas under the curve were determined.

2.8. Histology

Paraffin-embedded liver sections were stained with H&E. Frozen liver sections were stained with Oil red O (Sigma—Aldrich) to assess liver steatosis. Sections were rinsed in distilled water and 70% isopropyl alcohol, stained with Oil red O for 10 min, rinsed again in 70% isopropyl alcohol followed by washing in distilled water 3 times for 5 min and counterstaining with hematoxylin (Vector Laboratories). Fibrosis was determined by staining collagen content with Sirius Red. Formalin-fixed paraffin-embedded liver sections were deparaffinized, rehydrated, stained for 30 min with Sirius Red/Fast Green collagen kit (Chondrex, #9046), dehydrated, and mounted with Permount (Sigma—Aldrich, #SP15-100) [27]. Sirius Red and Oil-Red-O positive staining were quantified using ImageJ as percentage area stained per 20× field. Liver histology was assessed by an expert liver pathologist in a blinded manner.

Cell proliferation was determined by staining paraffin-embedded liver sections with an antibody for Ki67 (1:400; #CST12202) and imaged with the Leica Biosystems Bond RX staining system. For α-fetoprotein (AFP) staining, the formalin-fixed/paraffin-embedded sections were deparaffinated with Histoclear (National Diagnostics; #HS-200) and rehydrated by a series of ethanol solutions (100%, 90%, 80%, and 70%), and then with 100% PBS. The sections were then placed in an antigen retrieval buffer (containing 10 mM sodium citrate, 0.05% Tween-20, pH 6.0) and heated at 95 °C for 20 min, rinsed in PBS and treated with 2% hydrogen peroxide for 20 min to quench endogenous peroxidase activity. The sections were rinsed in PBS and then blocked with 1.5% goat serum in PBS containing 0.1% Tween-20 (PBST) for 1 h at room temperature. Sections were incubated overnight with an anti-AFP antibody (diluted at 1:300, Proteintech #14550-1-AP) in blocking buffer and then thoroughly washed five times with PBST. Subsequently, they were treated with anti-rabbit biotinylated secondary antibody, followed by incubation with avidin and biotinylated-horseradish peroxidase (Vectastain Elite ABC kit from Vector Laboratories). Sections were exposed to peroxidase substrate diaminobenzidine [7]. Nuclei were counterstained with hematoxylin (Vector Laboratories #H-3401-500).

2.9. Immunoblotting

Frozen liver tissue (20 mg) was ground to powder and proteins extracted with sonication using a modified RIPA buffer (50 mM Tris base; pH 7.4, 1 mM EDTA, 150 mM NaCl, 0.1% sodium dodecyl sulphate, 1% Triton X-100, 1% sodium deoxycholate) containing HALT protease/phosphatase inhibitors (Thermo Fisher #78440. Liver homogenates were then centrifuged at 12,000 xG for 15 min at 4 °C and the supernatant collected. For nuclear extracts, 20 mg of frozen tissue was dounce homogenized and processed as described using the Nuclear Extraction Kit (#ab113474). Proteins were measured with the Pierce BCA Protein Assay Kit (Thermo Fisher #23227). Equal amounts of protein were separated by 10% SDS-PAGE and transferred to 0.2 μm pore-size nitrocellulose (#1620112, BioRad) using the PierceG2 Fast Blotter (Thermo Fisher #62287). Blots were incubated with the following primary antibodies: Anti-p62 (#CST5114), anti-NQO1 (Abcam, #ab80588), anti-phospho-p62 S403 (#MABC186-I), anti-phospho-p62 S349 (#CST16177), anti-MYC (#CST13987), anti-CCND1 (#CST2978), anti-NRF2 (#CST12721), anti-HDAC1 (#34589), anti-β-tubulin (#CST2146), anti-β-actin (#CST3700), or GAPDH (#CST5174) and then incubated with secondary antibodies conjugated with horseradish peroxidase (goat anti-rabbit; 1:5000; Jackson ImmunoResearch, West Grove, Pa). Immunopositive bands were visualized using SuperSignal West Pico Stable Peroxide Solution or Dura Extended Duration Substrate (Thermo Scientific). Bands were quantified with ImageJ software and normalized to loading controls.

2.10. Immunofluorescence

Paraffin embedded liver sections were deparaffinized, subjected to antigen retrieval, and blocked with 5% Normal Serum Blocking Solution (Biolegend #927501), 1% BSA, and 0.4% Triton-X100 as previously described [7]. Subsequently, sections were incubated overnight with rabbit anti-p62 (Cell Signaling Technology, #CST5114S) at 1:200 in blocking buffer (PBS containing 5% normal goat serum (Thermo Fisher, #31872), 1% BSA, and 0.4% Triton X-100). Subsequently, sections were washed three times for 5 min with PBS, stained with goat anti-rabbit AlexaFluor 488 1:200 (Thermo Fisher, #A11008) in blocking buffer, washed three times for 5 min with PBS, and mounted with VECTASHIELD Vibrance antifade mounting medium containing DAPI (Vector Laboratories, #H-1800). Sections were imaged using a BZ-X810 Keyence fluorescence microscope. ImageJ was used to measure the percentage of p62 positive staining.

2.11. Cell imaging

After the indicated treatments, hepatocytes were briefly washed with ice-cold PBS followed by fixation with 4% PFA in PBS for 15 min and permeabilization with 0.1% Triton X-100 for 3 min, at room temperature. Hepatocytes were then incubated with blocking buffer (5% FCS and 1% BSA in PBS) for 30 min at room temperature before incubating overnight in a humidified chamber with anti-p62 (1:50, #CST5114) in blocking buffer at 4 °C. Cover slips were washed 3 times with ice-cold PBS before incubation with goat anti-rabbit Alexa Fluor 488 (1:100, #A11008) for 1 h at room temperature. Cells were then washed 3 times with ice-cold PBS and mounted with VECTASHIELD vibrance antifade mounting medium with DAPI (Vector Laboratories, #H-1800) onto glass slides.

Cells were imaged with an inverted Zeiss LSM880 confocal microscope with a 63× PlanApo oil immersion lens (numerical aperture 1.4). Fluorescence was excited using a 405 nm laser diode to excite DAPI and a 488 nm argon-ion laser to excite Alexa Fluor 488 for detection of endogenous p62. The confocal pinhole was set to 1 Airy unit for an emission wavelength of 520 nm. Emission of DAPI was detected in the wavelengths 410—470 nm and 490—550 nm for Alexa Fluor 488 to capture 16-bit images. Each image was thresholded to 10000—65535 to account for background fluorescence and particles were analyzed using the particle analysis tool in ImangeJ detecting a minimum size of 0.2 μm (minimum size of autophagasomes). For each group, 10 cells were quantified from 3 independent experiments and graphed as number of particles per cell and size of particles.

2.12. Hepatocyte isolation and culture

Mice were subjected to two-step collagenase perfusion for isolation of primary hepatocytes [28]. Briefly, mice euthanized with isoflurane were catheterized in the inferior vena cava and perfused through the liver and portal vein with HBSS containing 0.1% heparin (EMD Millipore, #375095), followed by perfusate 1 (8.3 g/L NaCl, 0.5 g/L KCl, 0.24 g/L Hepes, and 0.95 g/L EGTA pH 7.4), and perfusate 2 (10 g/L BSA (Thermo Fisher, #BP9704100), 3.9 g/L NaCl, 0.5 g/L KCl, 24 g/L

Hepes, and 0.7 g/L $CaCl_2$) with collagenase D (Sigma, #C6885). Digested tissue was filtered, centrifuged, washed with William's E media (Thermo Fisher, #12551032), and hepatocytes obtained by Percoll (Sigma #P1644) gradient centrifugation. After washing with William's E, cells were plated and cultured overnight in William's E media containing 1% penicillin/streptomycin, 2 mM L-glutamine, 15 mM Hepes, 1.16 mg/mL insulin (Santa Cruz, #sc-360248), 0.5 μM dexamethasone, and 10% fetal bovine serum (FBS). Viability of isolated hepatocytes was around 90%.

2.13. Fatty acid treatment of hepatocytes

Primary hepatocytes were plated at 4×10^5 cells per well onto collagen coated 6-well plates. For fatty acid treatments, 100 mM palmitate (PA) (Sigma, #P5585-10G) dissolved in ethanol was first heated to 70 °C and added dropwise to 5% fatty acid free BSA (Thermo Fisher, #BP9704100) dissolved in DMEM media without FBS at 55 °C to make a 5 mM PA/5% BSA stock solution. Ethanol/5% BSA solutions were used for vehicle control treatments. Cells were treated with the 500 μM PA and 0.7% BSA in DMEM containing penicillin/streptomycin, L-glutamine, and sodium pyruvate for 20 h. For sex hormone treatments, phenol-free DMEM was used with 500 μM PA/0.5% BSA and either 10 nM 5α-dihydrotestosterone (DHT) (Sigma, #D-073-1ML) or 100 nM β-estradiol (Sigma, #E8875-250 MG) for 20 h. Methanol or ethanol solutions were used as controls for the addition of the sex hormones in these vehicles. For immunoblotting, hepatocytes were washed in ice-cold PBS and proteins extracted with a modified RIPA buffer (50 mM Tris, 1 mM EDTA, 150 mM NaCl, 0.1% SDS, 1% Triton X-100, 1% sodium deoxycholate). Equal amounts of protein were separated by SDS-PAGE and immunoblotted as described above.

2.14. Quantitative real-time PCR

Quantitative real-time PCR was conducted as described previously [26]. Primer sequences used for human SphK2 were forward 5′-CCAGTGTTGGAGAGCTGAAGGT-3′ and reverse 5′-GTCCATTCATCTGC TGGTCCTC-3'. The internal control sequences for 18S ribosomal RNA were forward 5′-GTAACCCGTTGAACCCCATT-3′ and reverse 5′-CCATC CAATCGGTAGTAGCG-3'. SphK2 mRNA expression was quantified relative to 18S ribosomal RNA using the $2^{-\Delta\Delta Ct}$ method (Applied Biosystems).

2.15. Statistical analysis

Statistical significance was determined using unpaired two-tailed Student's t-test with Welch's correction for comparison of two groups, or by ANOVA followed by post hoc tests for multiple comparisons using GraphPad Prism 7.0. For all experiments, the normality of the data from each group was first checked using the Shapiro—Wilk statistical test. For non-normally distributed data, the Mann—Whitney U test was used. The following designations for significance levels are $*p < 0.05$, $**p < 0.01$, and $***p < 0.001$.

3. RESULTS

3.1. Deletion of SphK2 protects both males and females from western diet-induced metabolic dysfunction

To investigate the involvement of SphK2 in MASH-driven HCC, wild type and SphK2$^{-/-}$ male and female mice were fed chow diet (CD) or a high fat, cholesterol and carbohydrate diet with access to high glucose and fructose sugar water which was previously shown to recapitulate a typical western diet (WD) and reliably mimic key pathophysiological, metabolic, transcriptomic, histologic changes, and clinical outcomes of MASH-associated HCC found in human patients [7]. Male and female WT mice on WD gained weight, had increased accumulation of epididymal visceral white adipose tissue (eWAT), and developed enlarged livers compared to mice fed CD (Figure 1A—C). WD also induced clinically relevant markers of liver damage determined by increased serum alanine and aspartate aminotransferase (ALT, AST) (Figure 1D,E) and led to glucose intolerance (Figure 1F), which is highly associated with increased risk for MASH [29]. SphK2 deletion had no effect on CD fed mice. However, SphK2 deletion in both male and female mice significantly reduced WD-induced weight gain, eWAT fat mass, ALT/AST, and improved glucose intolerance (Figure 1A—F), suggesting that SphK2 deletion protects both sexes from diet-induced metabolic dysfunction.

Weight gain and metabolic dysfunction in WD fed WT mice were previously shown to be accompanied by gradual progression of increased liver steatosis, hepatocellular ballooning, inflammation, and bridging fibrosis [7], clinically relevant histological indications of human MASH [5,29]. Marked increases in steatosis, determined by neutral lipid Oil Red O staining of lipid accumulation, were similar in both sexes of WT and Sphk2$^{-/-}$ mice fed WD (Figure 2A,B). Pericellular and bridging liver fibrosis, was significantly elevated especially in males compared to females (Figure 2A,C). Although SphK2 deletion reduced liver damage (Figure 1D), nevertheless, it did not reduce the extent of WD-induced fibrosis in either males or females (Figure 2A,C). Even though the mechanism for the transition from MASH to HCC is not completely understood, it has been reported that chronic liver damage during the development of MASH is associated with a compensatory increase in hepatocyte proliferation [3,7,30] a critical process in hepatocarcinogenesis [31]. Significant increases of Ki67 positive hepatocytes were observed in livers from WD fed WT mice compared to those from CD fed mice, especially in males compared to females (Figure 2D). Consistent with a previous study with male mice [18], in Sphk2$^{-/-}$ livers, the numbers of hepatocytes positive for the proliferation marker Ki67 were decreased compared to WT, albeit not statistically significant (Figure 2D). Such an effect was not observed in livers from Sphk2$^{-/-}$ female mice (Figure 2D).

3.2. SphK2 deletion reverses the sexual dimorphism of liver cancer

Chronic WD feeding leads to a gradual progression from MASH to spontaneous HCC [3,7]. We previously reported that 75% of WD fed WT male mice for 54 weeks developed liver tumors, half of which were HCC as shown by positive staining for the HCC marker α-fetal protein (AFP) [7]. In agreement, tumors were almost absent in CD fed WT males with only a single mouse displaying a tumor (1/16 mice), whereas 78% of chronic WD fed mice developed tumors (22/28 mice), and among those, 80% had tumors larger than 1 mm and 55% had tumors larger than 5 mm, resulting in a significant increase in tumor burden (Figure 3A—D). Tumor incidence was significantly reduced in SphK2$^{-/-}$ male mice fed WD compared to WT, with 55% developing tumors (12/22 mice), along with a marked reduction in tumor size and tumor burden with only 19% having tumors larger than 5 mm (Figure 3A,B). Similar to the reduced liver cancer incidence found in human females [2,32], no tumors were detected in livers of WT females on either CD (0/14 mice) or WD (0/18 mice) (Figure 3A,B). Remarkably, SphK2 deletion in females fed WD increased liver cancer development with 40% developing tumors (6/15 mice) and 27% of those having a tumor greater than 1 mm (Figure 3A—D). In accordance with the tumor load observed in these mice (Figure 3A—D), the hepatic

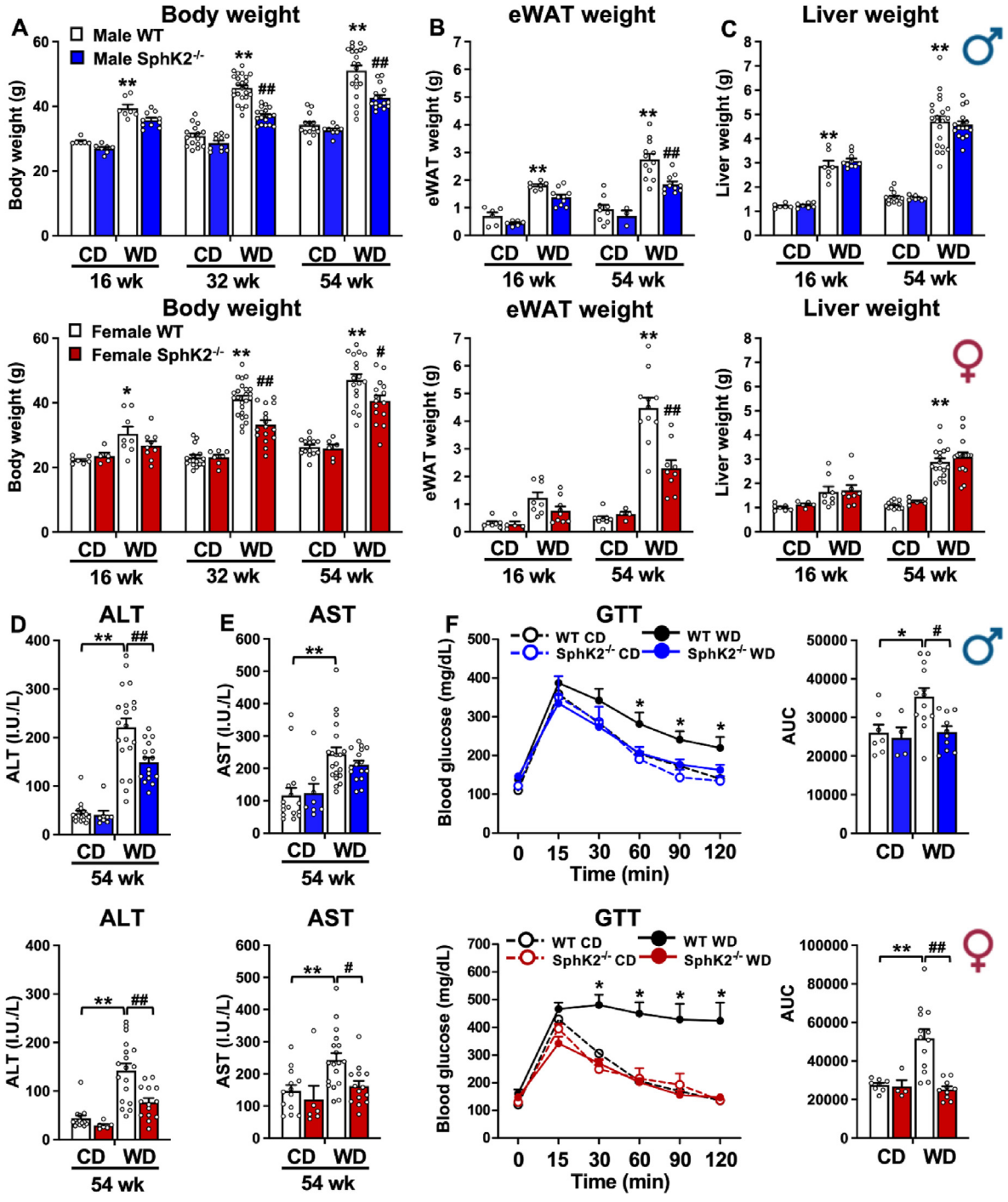

Figure 1: Deletion of SphK2 protects both sexes from Western diet-induced metabolic dysfunction. WT and SphK2$^{-/-}$ male and female mice were fed chow diet (CD) or high fat and cholesterol diet with high fructose/glucose drinking water (Western diet, WD) for 16, 32, or 54 weeks. (A) Body weights (16 wk n = 6–10 mice/group, 32 wk n = 10–24 mice/group, 54 wk n = 8–21 mice/group). (B) Epididymal while adipose tissue mass (eWAT) (16 wk = 5–10 mice/group, 54 wk n = 3–12 mice/group). (C) Liver weights (16 wk n = 5–10 mice/group, 54 wk n = 6–21 mice/group). (D,E) ALT and AST assays (n = 6–20 mice/group). (F) Glucose tolerance tests (n = 4–13 mice/group). Data are mean ± SEM. *$p < 0.05$, **$p < 0.01$ compared to respective WT fed CD. #$p < 0.05$, ##$p < 0.01$ compared to respective WT fed WD. (A–C) Two-way analysis or (D–F) one-way analysis of variance test followed by Tukey's multiple comparison test.

nodules had increased AFP expression with loss of hepatic architecture confirming the presence of HCC solely in livers from obese females lacking SphK2 (Figure 3E). Together, these results suggest that SphK2 ablation reverses the sexually dimorphic susceptibility of diet-induced liver cancer in mice.

3.3. SphK2 deficiency reduces p62 accumulation only in obese male mice

Obesity is associated with autophagy inhibition [33], leading to accumulation of the signaling adaptor and ubiquitin binding autophagy receptor p62 (encoded by the SQSTM1 gene) [34] that is required for

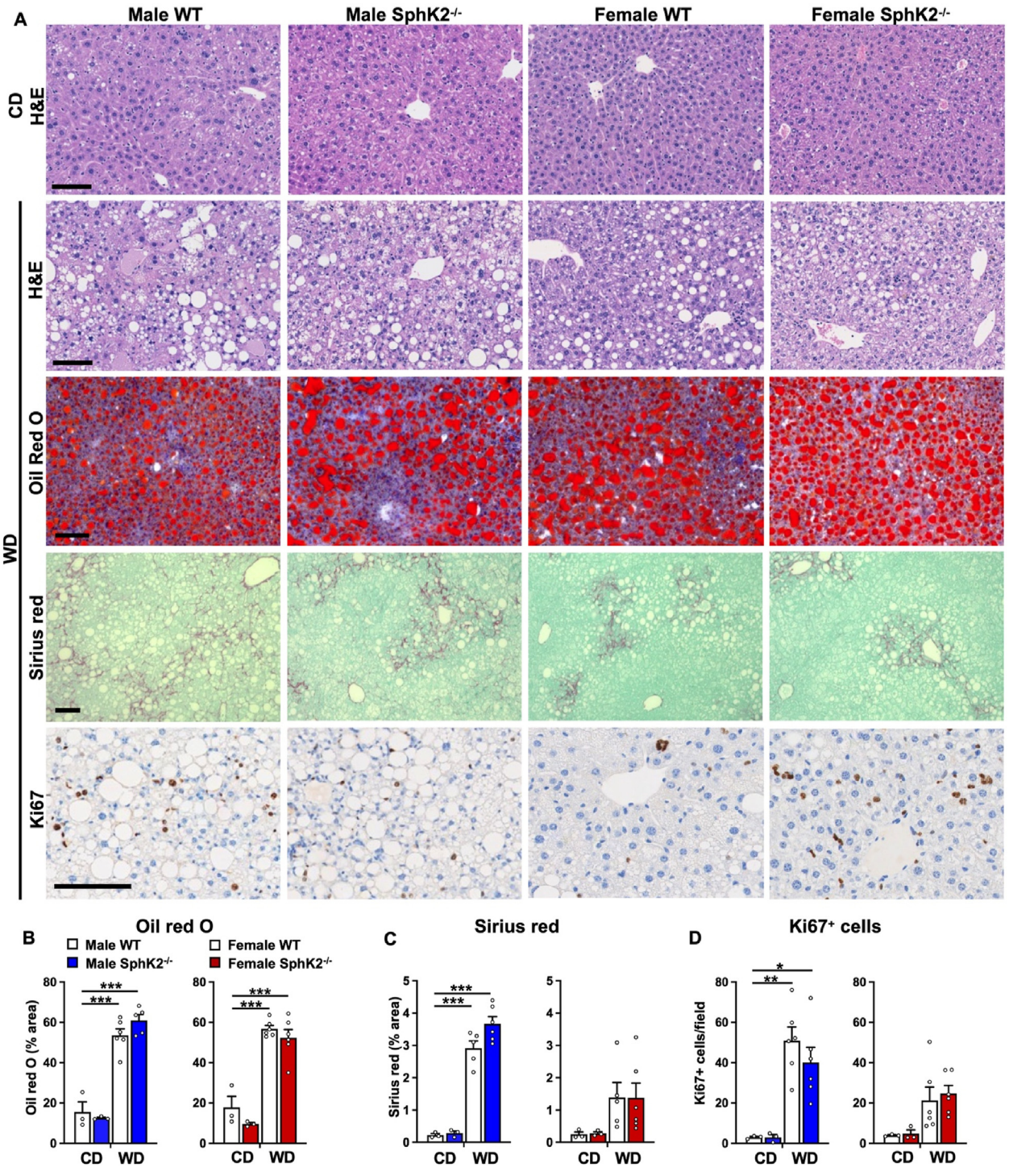

Figure 2: Lack of effect of SphK2 deletion on lipid accumulation or fibrosis in WD fed mice. (A) Representative images of liver sections from WT and SphK2$^{-/-}$ male and female mice fed CD or WD for 54 weeks stained with H&E, Oil red O, Sirius red/fast green, or anti-Ki67 antibody. Scale bars: 100 μm. (B,C) Oil red O and Sirius red staining for each mouse was quantified as average percent staining per total tissue surface area. CD, n = 3 mice/group; WD, n = 5–6 mice/group). (D) Quantification of average number of Ki67 positive cells per field in each mouse (CD, n = 3 mice/group; WD, n = 6 mice/group). Data are mean ± SEM. $^{**}p < 0.01$, $^{***}p < 0.001$ compared to respective WT fed CD. $^{\#\#}p < 0.05$, $^{\#\#}p < 0.01$, $^{\#\#\#}p < 0.001$ compared to WT fed WD. One-way analysis of variance test followed by Tukey's or Dunn's multiple comparison test.

premalignant progression of hepatocytes to HCC, and is elevated in human MASH and HCC liver samples [6,35]. Therefore, we sought to compare p62 levels in obese male and female mice and to evaluate the effects of SphK2 deletion. CD feeding of WT male mice, which do not develop HCC, did not induce p62 accumulation (Figure 4A). However, as in non-tumor liver biopsies from human patients with resectable HCC [6], chronic WD feeding induced strong p62 expression in non-tumor liver tissues of male mice (5–36-fold) (Figure 4A) and in the

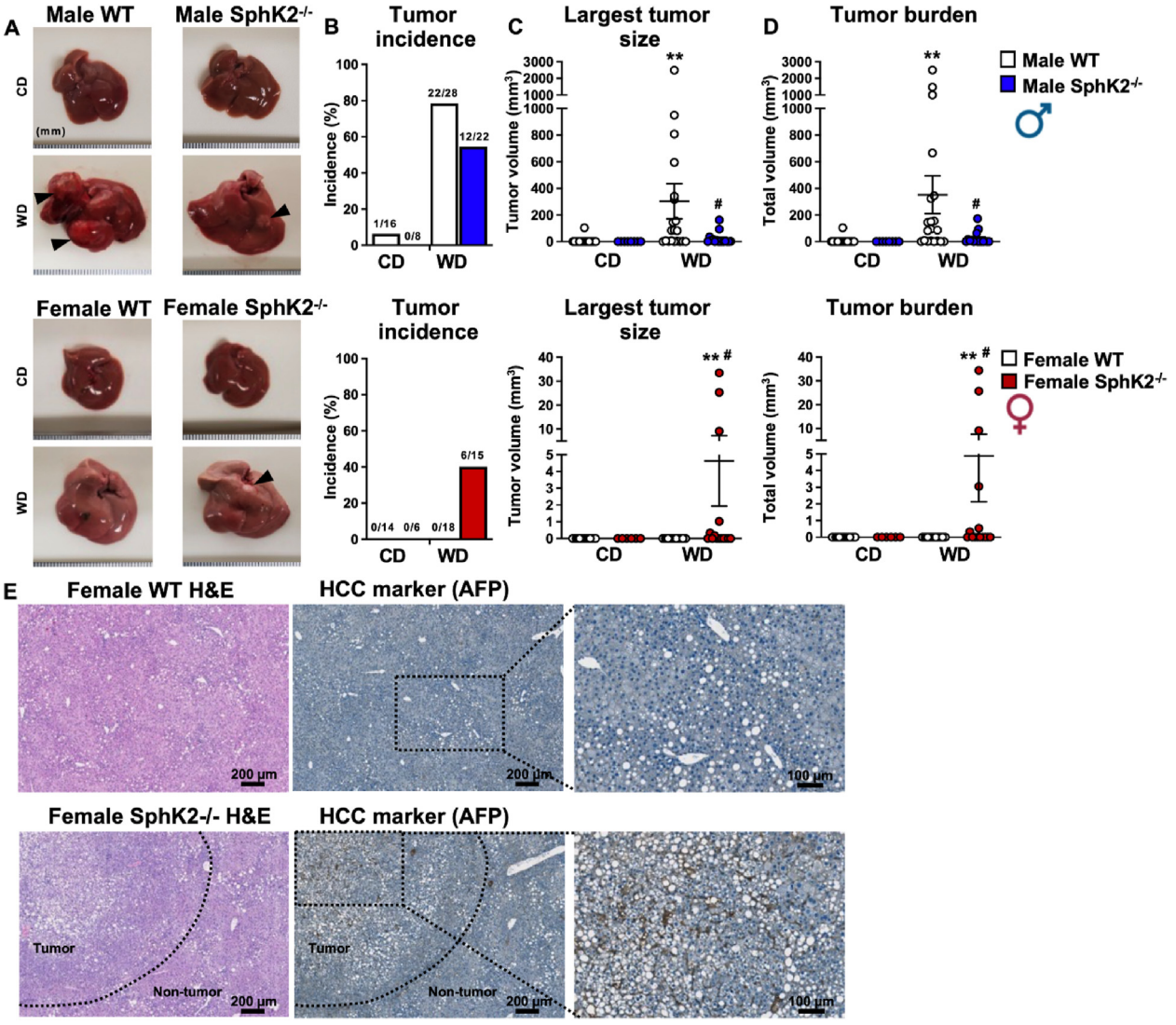

Figure 3: SphK2 deletion protects males from WD-induced HCC, but promotes it in females. (A) Representative liver images of WT and SphK2$^{-/-}$ male and female mice fed CD or WD for 54 weeks. Arrows indicate liver tumors. (B) Liver tumor incidence. (C) Largest tumor size. (D) Total tumor burden. n = mice/group as indicated in B. Data are mean ± SEM and represent 3 independent experiments. $^{**}p < 0.01$ compared to WT fed CD, one-way analysis of variance test followed by Dunn's multiple comparison test. $^{\#}p < 0.05$ compared to respective WT fed WD, Welch's t-test. (E) Representative immunohistochemical staining for tumor marker AFP in female tumor and non-tumor tissue. Scale bars: 200 and 100 µm (image insets). Dotted line indicates tumor boundary.

tumors (Figure 4E). There was a small but not significant increased trend in WD fed female mice (Figure 4A). SphK2 deletion significantly repressed WD-mediated p62 induction in males determined by hepatic western blotting and confirmed by immunofluorescence staining of p62 (67 % reduction) (Figure 4A,B). In contrast, deletion of SphK2 did not affect hepatic p62 levels in females (Figure 4A,B).

Accumulation of p62 increases nuclear localization of the transcription factor, nuclear factor erythroid 2 (NRF2) that subsequently enhances expression of the antioxidant protein, NAD(P)H dehydrogenase quinone 1 (NQO1), important for tumor metabolism and malignant progression [6,36]. Consistent with these studies, WD feeding increased *NQO1 only in males and SphK2 deletion suppressed this increase* (Figure 4A). Both p62 phosphorylation at S403 related to diet and lipotoxicity-induced autophagic defect [37] and phosphorylation at S351 (S349 in humans) required for increased NRF2 activity [35] were also elevated in WT livers and repressed by the absence of SphK2 (Figure 4C). Moreover, there was a trend for reduced nuclear localization of NRF2 in SphK2 deleted male mice fed WD compared to WT (Figure 4D). Consistent with previous studies [6,38], western blotting confirmed that most tumors in male WT mice fed WD displayed high p62 expression, which was also seen in non-tumor areas, and were drastically reduced by SphK2 deletion (Figure 4E).

Other key mediators induced by p62 accumulation include the oncogene c-Myc, a known driver of HCC development [39], and Cyclin D1 that initiates HCC development by promoting cell-cycle progression [40]. While liver tumors had markedly increased c-Myc levels (4-fold) compared to non-tumor tissue, c-Myc was significantly suppressed in tumors from SphK2$^{-/-}$ livers (Figure 4F). Likewise, Cyclin D1 was up-regulated 8-fold in WT tumors and repressed with SphK2 deletion (Figure 4F).

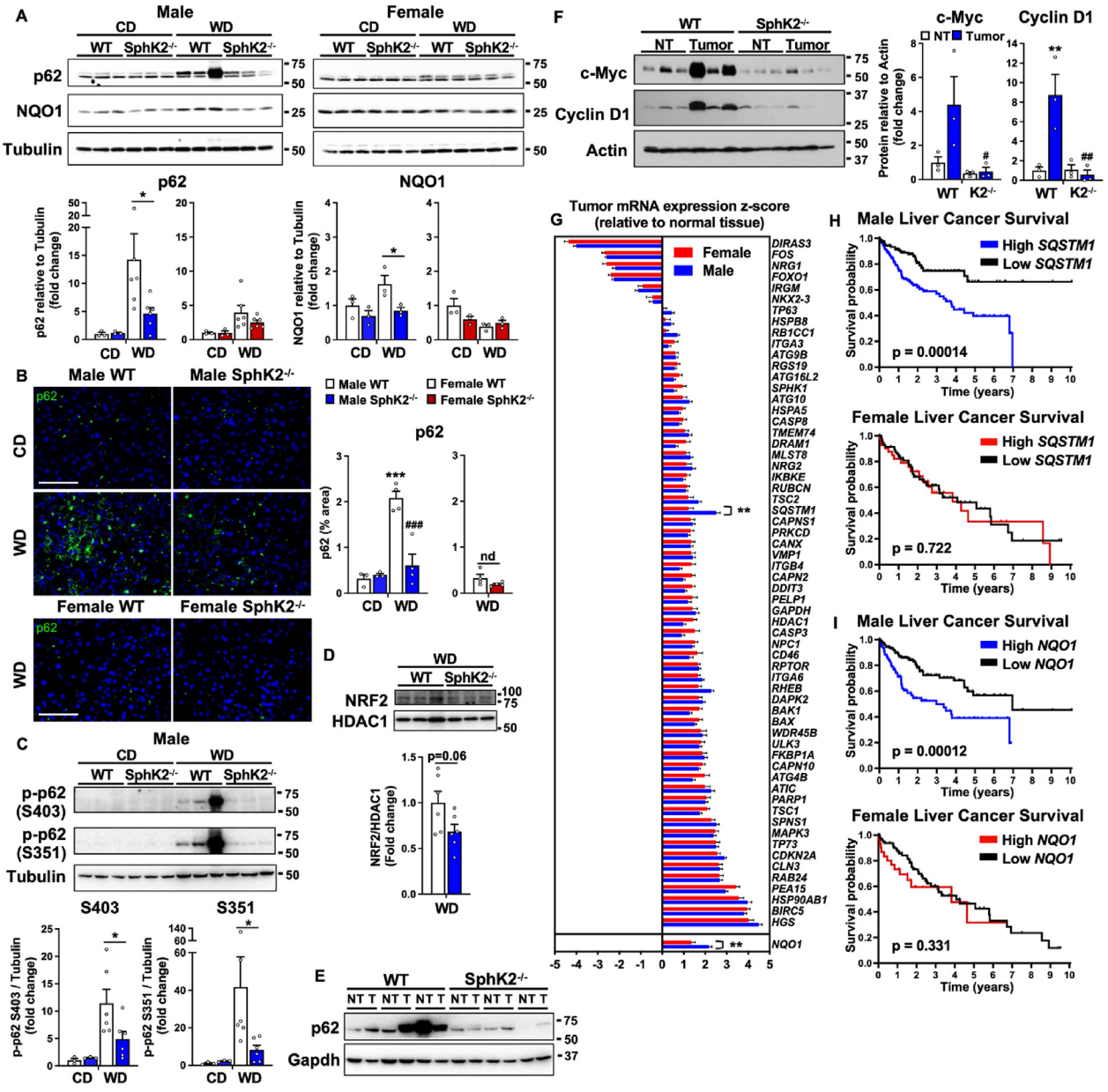

Figure 4: Chronic WD induced elevated p62 in male mice is repressed by SphK2 deletion and high p62 expression correlates with poor survival only in male HCC patients. (A) Immunoblot and quantitation of p62 (top band) and Nqo1 protein levels of non-tumor liver tissues from WT and SphK2$^{-/-}$ male and female mice fed CD or WD for 54 weeks. Data are mean ± SEM. *$p < 0.05$ compared to respective WT fed WD. (B) Representative immunofluorescent images and quantification of p62 in liver sections. Scale bar: 100 μm. Data are mean ± SEM. ***$p < 0.001$ compared to respective WT fed CD. $^{###}p < 0.001$ compared to respective WT fed WD. nd, no difference. (C,D) Immunoblot and quantification of p62 phosphorylation at S403 and S351 and nuclear levels of NRF2. Data are mean ± SEM. *$p < 0.05$ compared to respective WT fed WD. (A–D) CD, n = 3 mice/group; WD, n = 3–6 mice/group. Dots indicate individual mice. One-way analysis of variance test followed by Bonferroni's multiple comparison test. (E) Immunoblot of p62 levels in non-tumor (NT) and tumor tissue (T) from male mice fed WD for 54 weeks. (F) Immunoblot and quantification of c-Myc and Cyclin D1 protein levels in non-tumor (NT) and tumor tissue (T) from male mice fed WD for 54 weeks. **$p < 0.01$ compared to NT. $^{#}p < 0.05$, $^{##}p < 0.01$ compared to WT with tumor. NT and tumor, n = 3 mice/group. One-way analysis of variance test followed by Tukey's multiple comparison test. (G) Relative z-score normalized mRNA expression of 62 differentially expressed autophagy-related genes and *NQO1* in human liver tumors relative to normal tissue from females (n = 120) and males (n = 246). **$p < 0.01$ compared to female samples. Two-way analysis of variance test with Bonferroni's multiple comparison test. (H,I) Sex-specific survival analysis for in patients with HCC. Kaplan–Meier disease-free survival curves of male and female patients with HCC stratified by *p62/SQSTM1* or *NQO1* mRNA levels (z-score) from the TCGA PanCancer Atlas. Log rank test p-values.

3.4. Increased p62 correlates with poorer survival in male but not female HCC patients

Deregulation of autophagy has been proposed to play a key pathogenic role in HCC [33,41]. The sex dimorphisms in p62 expression we observed in diet-induced HCC in mice prompted us to examine whether there is sex-specific expression of p62 and other autophagy-related genes in human patients with HCC. A set of autophagy-related genes that are significantly differentially expressed in human HCC compared to non-tumor tissues [42] were analyzed by gender. Interestingly, only *p62* encoded by the *SQSTM1* gene was significantly higher in male tumors compared to females, whereas no or minimal changes were found for all the other 61 autophagy-related genes

(Figure 4G). Likewise, significantly increased expression of *NQO1* was noted in male but not female HCC patients (Figure 4G).

We next investigated whether *p62* and *NQO1* expression was associated with survival outcome among male and female patients with HCC. In accord with previous gender-inclusive studies [6,43], disease-free survival was significantly decreased in male patients with high expression of p62/SQSTM1 or NQO1 (Figure 4H,I). Nevertheless, the expression of these two genes was not associated with the survival of female patients with HCC (Figure 4H,I). Together, these findings suggest that activation of the p62/NQO1 pathway in mice and humans with HCC is much higher in males than in females and may contribute to reduced survival, particularly in males.

3.5. Modulation of lipotoxicity-mediated p62 accumulation by sex hormones in hepatocytes is repressed by SphK2 deletion

To further assess the involvement of SphK2 in p62 accumulation in response to lipotoxicity, we treated primary hepatocytes with palmitate (PA), which is the most common saturated fatty acid found in humans on a high fat diet [44]. Moreover, PA induced formation of p62 inclusion bodies in hepatocytes due to attenuation of autophagic flux [37]. Hepatocytes were treated with 500 μM PA, a level within the pathophysiological range [44], that was previously reported to induce p62 accumulation in hepatocytes [37,45,46]. In line with these reports, PA markedly increased p62 aggregate size and number in WT hepatocytes (Figure 5A,B), supporting the notion that PA impairs the final step of autophagy at the stage of autophagosome-lysosome fusion [37,45]. Similar to our observations *in vivo* (Figure 4A,B), in response to PA, hepatocytes with SphK2 deletion had markedly blunted p62 aggregates (Figure 5A,B), known to be present in human and rodent HCC [6,47–49].

The sexual dimorphism of HCC incidence and tumor growth has been suggested to involve differential actions of sex hormones, whereby female protection from HCC involves estrogen signaling and male susceptibility to HCC is linked to androgen signaling [2,4,50,51]. Therefore, we examined the effects of sex hormones on lipotoxicity-induced p62 aggregation. Interestingly, in WT hepatocytes the endogenous androgen 5α-dihydrotestosterone (DHT) significantly increased p62 aggregate size and number, effects that were suppressed by SphK2 deletion (70% in size, 96% in number) (Figure 5C). In contrast, activation of estrogen signaling with β-estradiol (E2) significantly reduced PA-induced p62 aggregate size (53%) and number (91%) and SphK2 deletion did not further decrease the effects of estrogen (Figure 5D).

3.6. High SphK2 expression in male human liver cancer patients is associated with poor differentiation status and increased risk of cancer recurrence

To examine the relevance of SphK2 expression in human HCC patients, we assessed its expression in tumor and non-tumor samples from the TCGA database and from an independent cohort of patients prior to surgical resection. In both cohorts, SphK2 mRNA was elevated in liver tumors from both male and female patients compared with adjacent normal tissue (Figure 6A,B). We then determined the differentiation status of the tumors, which is known to correlate with their aggressiveness [52]. Tumors were stratified as either more aggressive with poorly differentiated status, moderately differentiated, or well differentiated status. High SphK2 expression was only present in the more aggressive poorly differentiated tumors in males but not in females (Figure 6C). To analyze the correlation between high SphK2 and cancer outcome, we divided these patients based upon SphK2 expression and assessed the risk of cancer recurrence after resection of the tumor. Intriguingly, high SphK2 expression in tumors prior to surgery was significantly associated with both intra- and extra-hepatic recurrence of cancer in male patients (Figure 6D). In contrast, there was no significant difference in cancer recurrence in female patients based on levels of SphK2 (Figure 6E). These findings suggest that SphK2 expression may serve as an additional biomarker for assessing the risk of HCC recurrence in males and to distinguish patients who require vigilant monitoring after curative HCC ablation.

4. DISCUSSION

Gender disparity in HCC is well established, yet studies identifying the mechanisms that account for this difference and also lead to gender-specific therapeutic treatments are still lacking. We uncovered a previously unrecognized sex-specific role of SphK2 whereby it promotes HCC in males and is protective for females in mice and humans. Although SphK2 deletion strikingly reversed the sex differences in WD-induced tumor incidence, and tumor burden, we found reduced body weight and adipose tissue mass and improved glucose tolerance in both male and female SphK2 deficient mice fed WD. It was also recently reported that hepatocyte-specific SphK2 deletion increased insulin resistance and glucose intolerance [16]. However, changes in glucose and insulin resistance in mice have no apparent roles in HCC development [30]. Moreover, although MASH is generally associated with obesity and related HCC comorbidities, lean individuals with MASH, but with normal glucose tolerance, can still develop liver cancer [53], and mice fed different types of high fat and sugar diets produced varying levels of tumor burden without correlation to glucose tolerance [54].

Despite sex-specific effects of SphK2 on chronic diet-induced HCC development, SphK2 deletion did not affect the extent of WD-induced steatosis and fibrosis in either males or females. Consistent with this unexpected observation, it was previously reported that deletion of the T cell protein tyrosine phosphatase (TCPTP) in hepatocytes also markedly accelerated HCC in mice treated with a chemical carcinogen that promoted HCC without affecting MASH or fibrosis [55]. Although the prevalent view that HCC must be predicated by the development of MASH with advanced fibrosis or cirrhosis [56], evidence has accumulated for the dissociation of MASH and fibrosis with HCC in obesity. Approximately 50% of MASH patients develop HCC before the onset of cirrhosis [53]. In fact, in individuals with metabolic syndrome, HCC may even manifest in the presence of simple steatosis, devoid of any MASH-related inflammation or fibrosis [57]. Nevertheless, only a few pathways that contribute to the development of HCC in the absence of MASH or evident fibrosis or cirrhosis have been fully investigated [55]. Defining the molecular mechanisms that govern the regulation of HCC initiation and progression by SphK2 in a gender-specific manner is critical for gaining a better understanding of processes involved in diet-induced progression of MASH to HCC and its sexual dimorphism. Intriguingly, deletion of SphK2 reduced accumulation of hepatic p62 in male but not female mice fed a WD. This is especially important since p62 elevation precedes HCC development in mice and humans, contributes to its development by enhancing survival of stressed HCC-initiating cells that allows them to acquire multiple oncogenic mutations, and p62 correlates with worse patient survival [6,58]. Our data suggests that SphK2 could be a regulator of p62 in males, which affects their susceptibility to liver cancer.

p62 is a multifunctional signaling hub that activates mTORC1-dependent induction of c-Myc [59] and NRF2, a transcription factor regulating expression of antioxidant enzymes such as NQO1 [6]. Levels of both Nqo1 and c-Myc as well as the proto-oncogene Cyclin D1 were

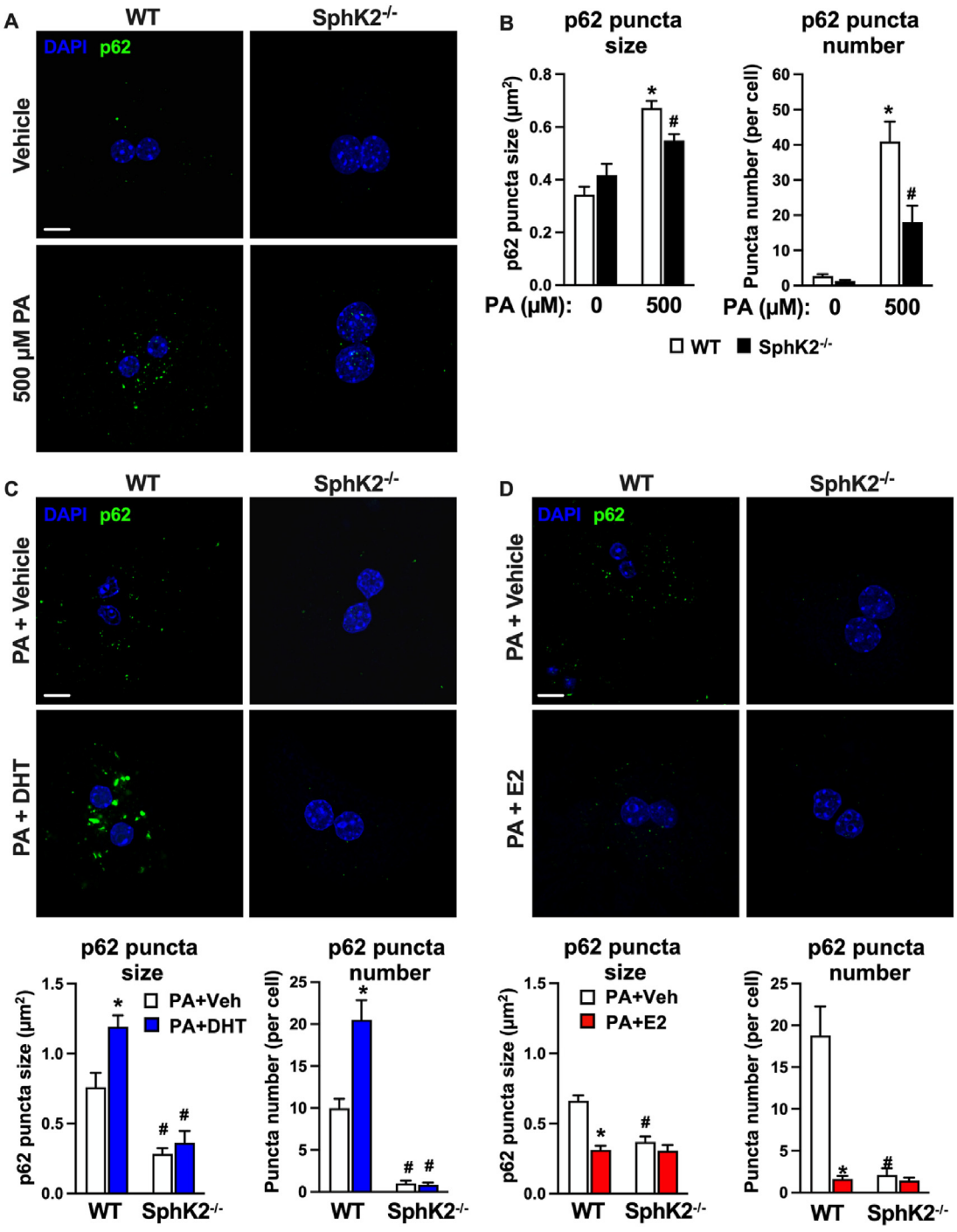

Figure 5: Lipotoxicity-induced p62 accumulation in hepatocytes is regulated by sex hormones and can be prevented by SphK2 deletion. (A,B) Representative confocal images and quantification of p62 aggregate size and number in WT and SphK2$^{-/-}$ primary hepatocytes treated with vehicle or 500 μM palmitate (PA). (C,D) Representative confocal images and quantification of p62 aggregate size and number in WT and SphK2$^{-/-}$ primary hepatocytes treated with vehicles or 500 μM PA in the absence or presence of dihydrotestosterone (DHT) or estradiol (E2). Scale bars: 10 μm. (B–D) Data are mean ± SEM from 3 independent experiments. *$p < 0.01$ compared to WT treated with vehicle. #$p < 0.05$ compared to respective WT hepatocytes treated with PA. One-way analysis of variance test followed by Tukey's multiple comparison test.

increased in tumors of WT male mice fed a WD and repressed by SphK2 deletion only in males. Thus, SphK2-mediated activation of the p62-NRF2-NQO1 pathway in HCC is predominately male-biased. Indeed, analysis of human HCC samples showed higher expression of *p62/SQSTM1* and *NQO1* in male tumors than in females. Moreover, high *p62/SQSTM1* and *NQO1* expression was associated with reduced survival of male patients, but there was no association for females. Importantly, we observed higher *SPHK2* expression in male tumors than those of females that was associated with a more aggressive HCC differentiation status. Furthermore, elevated *SPHK2* was associated with increased recurrence of intrahepatic and extrahepatic tumors after surgical resection, effects not observed in females, further

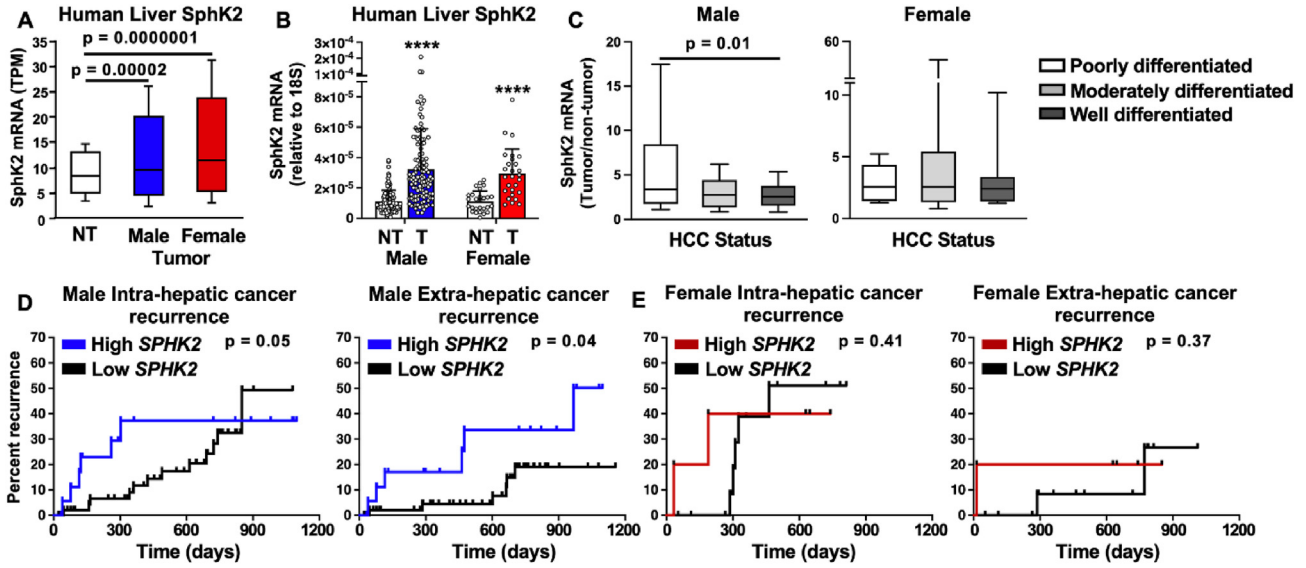

Figure 6: SphK2 expression in human sexual dimorphism of HCC. (A) SphK2 mRNA expression in liver tumors from male (n = 245) and female (n = 117) patients compared to normal tissue (n = 50) from TCGA. (B) Relative SphK2 mRNA levels determined by qPCR in non-tumor (NT) and tumor (T) samples from human male (n = 121) and female (n = 27) independent cohorts of patients. ****p < 0.0001 for T compared to NT. (C) SphK2 mRNA expression in male and female patients separated by HCC differentiation status defined as poorly, moderately, or well differentiated. p = 0.01 compared to poorly differentiated tumors. One-way analysis of variance test followed by Tukey's multiple comparison test. (D) SphK2 is a risk factor for cancer recurrence in males. Kaplan–Meier intra- and extra-hepatic recurrence curves were evaluated for male (n = 74) and female (n = 20) patients divided according to mRNA levels of SphK2. Survival analysis p values are indicated in the graphs.

suggestive of a role for SphK2 in promoting HCC in males. Our findings emphasize the need to analyze male and female survival data separately and indicate high *SPHK2*, *p62* and *NQO1* expression are linked to poor survival only in males. However, our study has some limitations. Since males are more likely to develop HCC, we were unable to collect a larger cohort of female patients, and the lower sample size may skew statistical significance. Nevertheless, in contrast to our findings in males, SphK2-mediated resistance of females to MASH-driven HCC is not dependent on p62. As HCC is influenced by the immune system especially in females [50,60,61], SphK2 may regulate the tumor immune microenvironment containing distinct immune cell populations associated with the progression or inhibition of HCC. Alternatively, as the liver is the main site where E2 is metabolized, SphK2 might affect expression of enzymes that metabolize it to suppress HCC [62]. Further studies are needed to determine the mechanism by which SphK2 suppresses MASH-driven HCC in females.

Autophagy impairment during obesity contributes to lipotoxicity and the pathogenesis of MASH-promoted HCC [34]. Modeling this effect by exposure of hepatocytes to the saturated fatty acid palmitate induced p62, its aggregation, and subsequent inhibition of autophagosome-lysosome fusion, in agreement with other reports [45,63,64]. Consistent with the notion that sex hormone signaling contributes to autophagy-mediated diseases [65] and to sexual dimorphism of HCC [2,4,50,51], we found that testosterone promotes p62 aggregation whereas estrogen reduces it. Notably deletion of SphK2 prevented p62 accumulation and aggregation. As SphK2 deletion reduces levels of S1P and increases levels of ceramide [66], which have been shown to induce autophagy through multiple mechanisms [67], it is tempting to speculate that changes in bioactive sphingolipid metabolites due to deletion of SphK2 could enhance autophagic fluxes and the autophagic clearance of p62 and thus contribute to reduced cancer initiation in males.

Although recent advances in animal models have characterized molecular and histopathological responses that mimic progression of MASH to HCC in humans, these studies have largely focused on males. Here, we reveal SphK2 as a potential new mediator of the sexual dimorphism of MASH-driven HCC. Our study has important clinical relevance for discovery of new drugs targeting SphK2, such as ABC294640/Opaganib (also called Yeliva) now in clinical trials for liver cancer (NCT01488513, NCT03377179, NCT04207255), as our findings suggest that it could have beneficial effects for males but deleterious effects for female patients, underscoring the importance of understanding sex differences in HCC.

ROLE OF THE FUNDING SOURCE

The funding source did not have any role in study design, data collection, data analyses, interpretation, or writing of report.

CREDIT AUTHORSHIP CONTRIBUTION STATEMENT

Christopher D. Green: Writing — review & editing, Writing — original draft, Funding acquisition, Formal analysis, Data curation, Conceptualization. **Ryan D.R. Brown:** Writing — review & editing, Data curation. **Baasanjav Uranbileg:** Writing — review & editing, Data curation. **Cynthia Weigel:** Writing — review & editing, Data curation. **Sumit Saha:** Writing — review & editing, Data curation. **Makoto Kurano:** Writing — review & editing, Data curation. **Yutaka Yatomi:** Writing — review & editing, Data curation. **Sarah Spiegel:** Writing — review & editing, Funding acquisition, Conceptualization.

ACKNOWLEDGMENTS

This work was supported by the National Institutes of Health under Grant R01CA266124 (C.D.G. and S.S.) and the VCU Accelerate Fund (C.D.G. and S.S.). We thank Justin Bettis from Virginia Commonwealth University School of Medicine for technical help with Ki67 staining. Services in support of this project were provided by the VCU Tissue and

Data Acquisition and Analysis Core and Microscopy Shared Resources, which were supported in part by funding to the Massey Cancer Center from the NIH-NCI Cancer Center Support Grant P30 CA016059.

DECLARATION OF COMPETING INTEREST

The authors declare that they have no known competing financial interests or personal relationships that could have appeared to influence the work reported in this paper.

DATA AVAILABILITY

Data will be made available on request.

REFERENCES

[1] Sung H, Ferlay J, Siegel RL, Laversanne M, Soerjomataram I, Jemal A, et al. Global cancer statistics 2020: GLOBOCAN estimates of incidence and mortality worldwide for 36 cancers in 185 countries. CA Cancer J Clin 2021;71(3):209–49.

[2] Li Y, Xu A, Jia S, Huang J. Recent advances in the molecular mechanism of sex disparity in hepatocellular carcinoma. Oncol Lett 2019;17(5):4222–8.

[3] Febbraio MA, Reibe S, Shalapour S, Ooi GJ, Watt MJ, Karin M. Preclinical models for studying NASH-driven HCC: how useful are they? Cell Metabol 2019;29(1):18–26.

[4] Li Z, Tuteja G, Schug J, Kaestner KH. Foxa1 and Foxa2 are essential for sexual dimorphism in liver cancer. Cell 2012;148(1–2):72–83.

[5] Friedman SL, Neuschwander-Tetri BA, Rinella M, Sanyal AJ. Mechanisms of NAFLD development and therapeutic strategies. Nat Med 2018;24(7):908–22.

[6] Umemura A, He F, Taniguchi K, Nakagawa H, Yamachika S, Font-Burgada J, et al. p62, upregulated during preneoplasia, induces hepatocellular carcinogenesis by maintaining survival of stressed HCC-initiating cells. Cancer Cell 2016;29(6):935–48.

[7] Green CD, Weigel C, Brown RDR, Bedossa P, Dozmorov M, Sanyal AJ, et al. A new preclinical model of western diet-induced progression of non-alcoholic steatohepatitis to hepatocellular carcinoma. Faseb J 2022;36(7):e22372.

[8] Chaurasia B, Tippetts TS, Mayoral Monibas R, Liu J, Li Y, Wang L, et al. Targeting a ceramide double bond improves insulin resistance and hepatic steatosis. Science 2019;365(6451):386–92.

[9] Chen J, Qi Y, Zhao Y, Kaczorowski D, Couttas TA, Coleman PR, et al. Deletion of sphingosine kinase 1 inhibits liver tumorigenesis in diethylnitrosamine-treated mice. Oncotarget 2018;9(21):15635–49.

[10] Tsang FH, Law CT, Tang TC, Cheng CL, Chin DW, Tam WV, et al. Aberrant super-enhancer landscape in human hepatocellular carcinoma. Hepatology 2019;69(6):2502–17.

[11] Montefusco D, Jamil M, Maczis MA, Schroeder W, Levi M, Ranjit S, et al. Sphingosine kinase 1 mediates sexual dimorphism in fibrosis in a mouse model of NASH. Mol Metabol 2022;62:101523.

[12] Nagahashi M, Takabe K, Liu R, Peng K, Wang X, Wang Y, et al. Conjugated bile acid activated S1P receptor 2 is a key regulator of sphingosine kinase 2 and hepatic gene expression. Hepatology 2015;61(4):1216–26.

[13] Lee SY, Hong IK, Kim BR, Shim SM, Sung Lee J, Lee HY, et al. Activation of sphingosine kinase 2 by endoplasmic reticulum stress ameliorates hepatic steatosis and insulin resistance in mice. Hepatology 2015;62(1):135–46.

[14] Song Z, Wang W, Li N, Yan S, Rong K, Lan T, et al. Sphingosine kinase 2 promotes lipotoxicity in pancreatic beta-cells and the progression of diabetes. Faseb J 2019;33(3):3636–46.

[15] Ravichandran S, Finlin BS, Kern PA, Ozcan S. Sphk2(-/-) mice are protected from obesity and insulin resistance. Biochim Biophys Acta, Mol Basis Dis 2019;1865(3):570–6.

[16] Aji G, Huang Y, Ng ML, Wang W, Lan T, Li M, et al. Regulation of hepatic insulin signaling and glucose homeostasis by sphingosine kinase 2. Proc Natl Acad Sci U S A 2020;117(39):24434–42.

[17] Shi Y, Wei Q, Liu Y, Yuan J. The alleviating effect of sphingosine kinases 2 inhibitor K145 on nonalcoholic fatty liver. Biochem Biophys Res Commun 2021;580:1–6.

[18] Liu XT, Chung LH, Liu D, Chen J, Huang Y, Teo JD, et al. Ablation of sphingosine kinase 2 suppresses fatty liver-associated hepatocellular carcinoma via downregulation of ceramide transfer protein. Oncogenesis 2022;11(1):67.

[19] Beljanski V, Lewis CS, Smith CD. Antitumor activity of sphingosine kinase 2 inhibitor ABC294640 and sorafenib in hepatocellular carcinoma xenografts. Cancer Biol Ther 2011;11(5):524–34.

[20] Antoon JW, White MD, Meacham WD, Slaughter EM, Muir SE, Elliott S, et al. Antiestrogenic effects of the novel sphingosine kinase-2 inhibitor ABC294640. Endocrinology 2010;151(11):5124–35.

[21] Engel N, Lisec J, Piechulla B, Nebe B. Metabolic profiling reveals sphingosine-1-phosphate kinase 2 and lyase as key targets of (phyto-) estrogen action in the breast cancer cell line MCF-7 and not in MCF-12A. PLoS One 2012;7(10):e47833.

[22] Zhang J, Zhang M, Huang J, Zhang G, Li C, Wang X, et al. Development and validation of an autophagy-related gene signature for predicting the prognosis of hepatocellular carcinoma. BioMed Res Int 2021;2021:7771037.

[23] Cerami E, Gao J, Dogrusoz U, Gross BE, Sumer SO, Aksoy BA, et al. The cBio cancer genomics portal: an open platform for exploring multidimensional cancer genomics data. Cancer Discov 2012;2(5):401–4.

[24] Chandrashekar DS, Bashel B, Balasubramanya SAH, Creighton CJ, Ponce-Rodriguez I, Chakravarthi B, et al. UALCAN: a portal for facilitating tumor subgroup gene expression and survival analyses. Neoplasia 2017;19(8):649–58.

[25] Chandrashekar DS, Karthikeyan SK, Korla PK, Patel H, Shovon AR, Athar M, et al. UALCAN: an update to the integrated cancer data analysis platform. Neoplasia 2022;25:18–27.

[26] Uranbileg B, Kurano M, Kano K, Sakai E, Arita J, Hasegawa K, et al. Sphingosine 1-phosphate lyase facilitates cancer progression through converting sphingolipids to glycerophospholipids. Clin Transl Med 2022;12(9):e1056.

[27] Lattouf R, Younes R, Lutomski D, Naaman N, Godeau G, Senni K, et al. Picrosirius red staining: a useful tool to appraise collagen networks in normal and pathological tissues. J Histochem Cytochem 2014;62(10):751–8.

[28] Seglen PO. Preparation of isolated rat liver cells. Methods Cell Biol 1976;13:29–83.

[29] Loomba R, Abraham M, Unalp A, Wilson L, Lavine J, Doo E, et al. Association between diabetes, family history of diabetes, and risk of nonalcoholic steatohepatitis and fibrosis. Hepatology 2012;56(3):943–51.

[30] Nakagawa H, Umemura A, Taniguchi K, Font-Burgada J, Dhar D, Ogata H, et al. ER stress cooperates with hypernutrition to trigger TNF-dependent spontaneous HCC development. Cancer Cell 2014;26(3):331–43.

[31] Maeda S, Kamata H, Luo JL, Leffert H, Karin M. IKKbeta couples hepatocyte death to cytokine-driven compensatory proliferation that promotes chemical hepatocarcinogenesis. Cell 2005;121(7):977–90.

[32] Bray F, Ferlay J, Soerjomataram I, Siegel RL, Torre LA, Jemal A. Global cancer statistics 2018: GLOBOCAN estimates of incidence and mortality worldwide for 36 cancers in 185 countries. CA Cancer J Clin 2018;68(6):394–424.

[33] Yang L, Li P, Fu S, Calay ES, Hotamisligil GS. Defective hepatic autophagy in obesity promotes ER stress and causes insulin resistance. Cell Metabol 2010;11(6):467–78.

[34] Moscat J, Karin M, Diaz-Meco MT. p62 in cancer: signaling adaptor beyond autophagy. Cell 2016;167(3):606–9.

[35] Ichimura Y, Waguri S, Sou YS, Kageyama S, Hasegawa J, Ishimura R, et al. Phosphorylation of p62 activates the Keap1-Nrf2 pathway during selective autophagy. Mol Cell 2013;51(5):618–31.

[36] Shimokawa M, Yoshizumi T, Itoh S, Iseda N, Sakata K, Yugawa K, et al. Modulation of Nqo1 activity intercepts anoikis resistance and reduces

metastatic potential of hepatocellular carcinoma. Cancer Sci 2020;111(4):1228–40.
[37] Cho CS, Park HW, Ho A, Semple IA, Kim B, Jang I, et al. Lipotoxicity induces hepatic protein inclusions through TANK binding kinase 1-mediated p62/sequestosome 1 phosphorylation. Hepatology 2018;68(4):1331–46.
[38] Saito T, Ichimura Y, Taguchi K, Suzuki T, Mizushima T, Takagi K, et al. p62/Sqstm1 promotes malignancy of HCV-positive hepatocellular carcinoma through Nrf2-dependent metabolic reprogramming. Nat Commun 2016;7:12030.
[39] Shibata T, Aburatani H. Exploration of liver cancer genomes. Nat Rev Gastroenterol Hepatol 2014;11(6):340–9.
[40] Wu SY, Lan SH, Wu SR, Chiu YC, Lin XZ, Su IJ, et al. Hepatocellular carcinoma-related cyclin D1 is selectively regulated by autophagy degradation system. Hepatology 2018;68(1):141–54.
[41] Schneider JL, Cuervo AM. Liver autophagy: much more than just taking out the trash. Nat Rev Gastroenterol Hepatol 2014;11(3):187–200.
[42] Zhu Y, Wang R, Chen W, Chen Q, Zhou J. Construction of a prognosis-predicting model based on autophagy-related genes for hepatocellular carcinoma (HCC) patients. Aging (Albany NY) 2020;12(14):14582–92.
[43] Li WY, Zhou HZ, Chen Y, Cai XF, Tang H, Ren JH, et al. NAD(P)H: quinone oxidoreductase 1 overexpression in hepatocellular carcinoma potentiates apoptosis evasion through regulating stabilization of X-linked inhibitor of apoptosis protein. Cancer Lett 2019;451:156–67.
[44] Richieri GV, Kleinfeld AM. Unbound free fatty acid levels in human serum. J Lipid Res 1995;36(2):229–40.
[45] Nissar AU, Sharma L, Mudasir MA, Nazir LA, Umar SA, Sharma PR, et al. Chemical chaperone 4-phenyl butyric acid (4-PBA) reduces hepatocellular lipid accumulation and lipotoxicity through induction of autophagy. J Lipid Res 2017;58(9):1855–68.
[46] Park JS, Kang DH, Lee DH, Bae SH. Concerted action of p62 and Nrf2 protects cells from palmitic acid-induced lipotoxicity. Biochem Biophys Res Commun 2015;466(1):131–7.
[47] Denk H, Stumptner C, Fuchsbichler A, Muller T, Farr G, Muller W, et al. Are the Mallory bodies and intracellular hyaline bodies in neoplastic and non-neoplastic hepatocytes related? J Pathol 2006;208(5):653–61.
[48] Inami Y, Waguri S, Sakamoto A, Kouno T, Nakada K, Hino O, et al. Persistent activation of Nrf2 through p62 in hepatocellular carcinoma cells. J Cell Biol 2011;193(2):275–84.
[49] Bartolini D, Dallaglio K, Torquato P, Piroddi M, Galli F. Nrf2-p62 autophagy pathway and its response to oxidative stress in hepatocellular carcinoma. Transl Res 2018;193:54–71.
[50] Clocchiatti A, Cora E, Zhang Y, Dotto GP. Sexual dimorphism in cancer. Nat Rev Cancer 2016;16(5):330–9.
[51] Zhang H, Li XX, Yang Y, Zhang Y, Wang HY, Zheng XFS. Significance and mechanism of androgen receptor overexpression and androgen receptor/mechanistic target of rapamycin cross-talk in hepatocellular carcinoma. Hepatology 2018;67(6):2271–86.
[52] Calderaro J, Ziol M, Paradis V, Zucman-Rossi J. Molecular and histological correlations in liver cancer. J Hepatol 2019;71(3):616–30.
[53] Younes R, Bugianesi E. NASH in lean individuals. Semin Liver Dis 2019;39(1):86–95.
[54] Healy ME, Chow JD, Byrne FL, Breen DS, Leitinger N, Li C, et al. Dietary effects on liver tumor burden in mice treated with the hepatocellular carcinogen diethylnitrosamine. J Hepatol 2015;62(3):599–606.
[55] Grohmann M, Wiede F, Dodd GT, Gurzov EN, Ooi GJ, Butt T, et al. Obesity drives STAT-1-dependent NASH and STAT-3-dependent HCC. Cell 2018;175(5):1289–1306 e1220.
[56] Font-Burgada J, Sun B, Karin M. Obesity and cancer: the oil that feeds the flame. Cell Metabol 2016;23(1):48–62.
[57] Alexander J, Torbenson M, Wu TT, Yeh MM. Non-alcoholic fatty liver disease contributes to hepatocarcinogenesis in non-cirrhotic liver: a clinical and pathological study. J Gastroenterol Hepatol 2013;28(5):848–54.
[58] Wang L, Hensley CR, Howell ME, Ning S. Bioinformatics-driven identification of p62 as A crucial oncogene in liver cancer. Front Oncol 2022;12:923009.
[59] Valencia T, Kim JY, Abu-Baker S, Moscat-Pardos J, Ahn CS, Reina-Campos M, et al. Metabolic reprogramming of stromal fibroblasts through p62-mTORC1 signaling promotes inflammation and tumorigenesis. Cancer Cell 2014;26(1):121–35.
[60] Hou J, Zhang H, Sun B, Karin M. The immunobiology of hepatocellular carcinoma in humans and mice: basic concepts and therapeutic implications. J Hepatol 2020;72(1):167–82.
[61] Mirshahi F, Aqbi HF, Isbell M, Manjili SH, Guo C, Saneshaw M, et al. Distinct hepatic immunological patterns are associated with the progression or inhibition of hepatocellular carcinoma. Cell Rep 2022;38(9):110454.
[62] Ren J, Chen GG, Liu Y, Su X, Hu B, Leung BC, et al. Cytochrome P450 1A2 metabolizes 17beta-estradiol to suppress hepatocellular carcinoma. PLoS One 2016;11(4):e0153863.
[63] Park HW, Park H, Semple IA, Jang I, Ro SH, Kim M, et al. Pharmacological correction of obesity-induced autophagy arrest using calcium channel blockers. Nat Commun 2014;5:4834.
[64] Hamlin AN, Basford JE, Jaeschke A, Hui DY. LRP1 protein deficiency exacerbates palmitate-induced steatosis and toxicity in hepatocytes. J Biol Chem 2016;291(32):16610–9.
[65] Shang D, Wang L, Klionsky DJ, Cheng H, Zhou R. Sex differences in autophagy-mediated diseases: toward precision medicine. Autophagy 2021;17(5):1065–76.
[66] Weigel C, Maczis MA, Palladino END, Green CD, Maceyka M, Guo C, et al. Sphingosine kinase 2 in stromal fibroblasts creates a hospitable tumor microenvironment in a p53-dependent manner. Cancer Res 2023;83:553–67.
[67] Young MM, Wang HG. Sphingolipids as regulators of autophagy and endocytic trafficking. Adv Cancer Res 2018;140:27–60.

